Uncovering Strong Lottery Tickets in Graph Transformers: A Path to Memory Efficient and Robust Graph Learning

Anonymous authors
Paper under double-blind review

Abstract

Graph Transformers (GTs) have recently demonstrated strong capabilities for capturing complex relationships in graph-structured data using global self-attention mechanisms. On the other hand, their high memory requirements during inference remain a challenge for practical deployment. In this study, we investigate the existence of strong lottery tickets (SLTs) — subnetworks within randomly initialized neural networks that can attain competitive accuracy without weight training — in GTs. Previous studies have explored SLTs in message passing neural networks (MPNNs), showing that SLTs not only exist in MPNNs but also help mitigate over-smoothing problems and improve robustness. However, the potential of SLTs in GTs remains unexplored. With GTs having 4.5× more parameters than MPNNs, SLTs hold even greater application value in this context. We find that fixed random weights with a traditional SLT search method cannot adapt to imbalances of features in GTs, leading to highly biased attention that destabilizes model performance. To overcome this issue and efficiently search for SLTs, we introduce a novel approach called Adaptive Scaling. We empirically confirm the existence of SLTs within GTs and demonstrate their versatility through extensive experiments across different GT architectures, including NodeFormer, GRIT, and GraphGPS. Our findings demonstrate that SLTs achieve comparable accuracy while reducing memory usage by 2–32×, effectively generalize to out-of-distribution data, and enhance robustness against adversarial perturbations. This work highlights that SLTs offer a resource-efficient approach to improving the scalability, efficiency, and robustness of Graph Transformers, with broad implications for applications involving graph data.

1 Introduction

Graph Neural Networks (GNNs) have achieved remarkable success in modeling graph-structured data across diverse domains such as social networks, biological networks, and recommendation systems (Fan et al., 2019; Choi et al., 2021; Wu et al., 2022b). By leveraging node connectivity and feature aggregation, GNNs excel at capturing local dependencies within graphs, enabling them to solve complex real-world tasks.

When it comes to modeling long-range dependencies, however, traditional GNNs—*a.k.a.* message passing neural networks (MPNNs)—face significant limitations. As MPNNs rely on iterative message passing between neighboring nodes, capturing interactions between distant nodes often requires stacking many layers, which leads to challenges such as over-smoothing (Li et al., 2018; Oono & Suzuki, 2020) and over-squashing (Topping et al., 2022; Di Giovanni et al., 2023).

Graph Transformers (GTs) have emerged as a powerful alternative to overcome the above problems, incorporating global self-attention mechanisms and achieving SOTA accuracy. Specifically, it allows nodes to attend to all other nodes in the graph. This global perspective enables GTs to effectively capture long-range dependencies, making them well-suited for tasks involving distant interactions across large and complex graphs.

Despite their high performance, GTs have the drawback of increased memory demands due to their multiple linear transformations during self-attention operations. For example, NodeFormer (Wu et al., 2022a) requires 4.59 times more memory than GCN (Kipf & Welling, 2017), and the linear layers at the GT layers take 89 %

of the model memory size. This resource intensity poses practical challenges for deploying these models in environments with limited hardware capacity. Moreover, when deploying GTs in real-world applications, robustness to perturbations (Zhu et al., 2024; Foth et al., 2024) and generalization to out-of-distribution (OOD) data (Li et al., 2022; Wu et al., 2023) are critical concerns. Models must be reliable in the face of noisy data and unexpected inputs.

To tackle these issues, network pruning techniques have been explored to reduce the model size while keeping competitive accuracy. Among these, the Strong Lottery Ticket Hypothesis (SLTH) (Zhou et al., 2019; Ramanujan et al., 2020; Malach et al., 2020) posits that within a randomly initialized neural network, there exist subnetworks—referred to as Strong Lottery Tickets (SLTs)—that can achieve competitive accuracy without any weight training. Recent work by Huang et al. (2022) demonstrated the existence of SLTs in MPNNs. It has also been observed that SLTs can mitigate over-smoothing, a common issue leading to accuracy loss in MPNNs, and enhance the robustness and OOD performance. However, it remains an open question **whether accurate SLTs exist within GTs**, and if so, **whether they offer benefits in perturbation and OOD challenges**.

In this work, we address these questions by investigating the existence of SLTs within GTs and their utility. During the investigation, we found that typical fixed random weights with a traditional SLT search method cannot adapt to distribution imbalances of activations, leading to highly skewed attention that destabilizes model performance. We introduce a novel approach incorporating Adaptive Scaling to overcome the challenges and effectively search for SLTs. Moreover, our proposed SLT methods not only reduce the memory footprint of GT but also enhance their robustness and generalization capabilities.

We conduct comprehensive experiments across two main kinds of GT architectures to validate our proposed approach: hybrid GTs (*e.g.*, GraphGPS (Rampášek et al., 2022)), which integrate MPNNs into GTs, and pure GTs (*e.g.*, NodeFormer (Wu et al., 2022a) and GRIT (Ma et al., 2023)), which do not have MPNNs. Our results empirically confirm the presence of SLTs in GTs and demonstrate that these subnetworks achieve comparable or even superior performance to trained dense models while significantly reducing memory usage. Furthermore, we show that SLTs enhance robustness against adversarial perturbations and improve generalization to OOD data. This finding is particularly significant for real-world applications where data is often noisy or deviates from the training distribution, and model reliability is important.

Our key contributions are summarized as follows:

- For the first time, we reveal the existence of SLTs in GTs by utilizing Adaptive Scaling methods, which combine Dynamic Weight Scaling (DWS) and Attention Stability Norm (ASNorm) to balance the attention scores and enhance training stability. Unlike the existing SLT search method (Ramanujan et al., 2020), which fails to identify lottery tickets in this context, our approach successfully uncovered them with $\geq 80\%$ sparsity.
- Our analysis reveals that the identified SLTs in GTs contribute to increased robustness against adversarial perturbations and improved generalization to OOD data. This highlights the potential of SLTs for building more reliable and safe GT models for practical applications.
- Our experiments cover both hybrid (with MPNN) and pure (without MPNN) GTs, evaluated on seven mainstream datasets for node-level tasks and six datasets for graph-level tasks. Compared to fully trained dense models, our approach achieves a 2–32$\times$ reduction in memory consumption while maintaining comparable accuracy and providing higher robustness.

2 Related Work

Graph Neural Networks: Graph Neural Networks (GNNs) are designed to learn optimal representations of graph-structured data, where nodes represent entities and edges capture the relationships between them. GNNs have been widely applied across various real-world domains, including social network analysis (Fan et al., 2019), recommendation systems (Wu et al., 2022b; Gao et al., 2022), drug discovery (Gaudelet et al., 2021), and autonomous driving(Choi et al., 2021). Graph Transformers (GTs) have emerged as an advanced

approach to GNNs. By leveraging the self-attention mechanism of Transformers, they can capture both local and global dependencies within a graph. Unlike MPNNs, which focus on aggregating information from local neighborhoods, GTs can attend to all nodes in the graph. This capability allows them to address the limitations of MPNNs like over-smoothing (Li et al., 2018; Oono & Suzuki, 2020) where node representations become indistinguishable, and over-squashing (Topping et al., 2022; Di Giovanni et al., 2023) where information from distant nodes is inadequately captured. They also perform better in tasks that require a global understanding of the graph structure, such as large graphs (Lerer et al., 2019; Xue et al., 2023) or time series data (Jiang & Luo, 2022; Zhang et al., 2022).

On the other hand, GTs face several significant challenges, particularly in terms of generalization (Li et al., 2022; Wu et al., 2023), robustness (Zhu et al., 2024; Foth et al., 2024), and memory demands (Ku, 2023). They often struggle to generalize to unseen graphs, especially when they have different distributions of features or classes during inference. Additionally, GTs are susceptible to adversarial attacks and noisy data, leading to decreased accuracy and unreliable results. Furthermore, their complex self-attention layers result in high memory demands, which can limit scalability in practical applications. Addressing these issues is essential for improving the applicability of GTs in real-world tasks.

Strong Lottery Ticket Hypothesis: The Lottery Ticket Hypothesis (Frankle & Carbin, 2019) proposes that within a dense neural network, there exist sparse subnetworks that, when trained in isolation, can achieve comparable or even higher accuracy than the original network. Building on this, Zhou et al. (2019) identified an even stronger phenomenon, the *Strong Lottery Ticket Hypothesis* (SLTH), which conjectures that accurate subnetworks exist within a randomly initialized network and can achieve comparable performance without any weight updates. However, it was difficult to identify such subnetworks due to the vast combinatorial search space, resulting in limited performance. To address this challenge, Ramanujan et al. (2020) introduced the Edge-Popup method, which efficiently searches for accurate subnetworks within randomly initialized networks without any weight training. Subsequent studies have confirmed the existence of strong lottery tickets experimentally (Zhou et al., 2021; Sreenivasan et al., 2022; Otsuka et al., 2024) and theoretically (Malach et al., 2020; Orseau et al., 2020; Pensia et al., 2020).

In the domain of GNNs, Huang et al. (2022) was the first to extend the SLTH to MPNNs. They explored the existence of SLTs within MPNNs and demonstrated their potential to address the over-smoothing problem (Li et al., 2018; Oono & Suzuki, 2020) and improve robustness (Zhu et al., 2024; Foth et al., 2024) and out-of-distribution (OOD) performance (Li et al., 2022; Wu et al., 2023). Additionally, Yan et al. (2024) advanced the application of SLTs in MPNNs by multicoating (Okoshi et al., 2022) and folding (García-Arias et al., 2023) supermasks, significantly reducing memory requirements while maintaining competitive accuracy. Collectively, these studies demonstrate the potential of SLTs in the context of MPNNs. However, **the existence and utility of SLTs within GTs remain unexplored**. Therefore, we aim to investigate whether SLTs can alleviate the memory limitations of GTs and enhance their robustness and generalization capabilities.

3 Strong Lottery Tickets within Graph Transformers

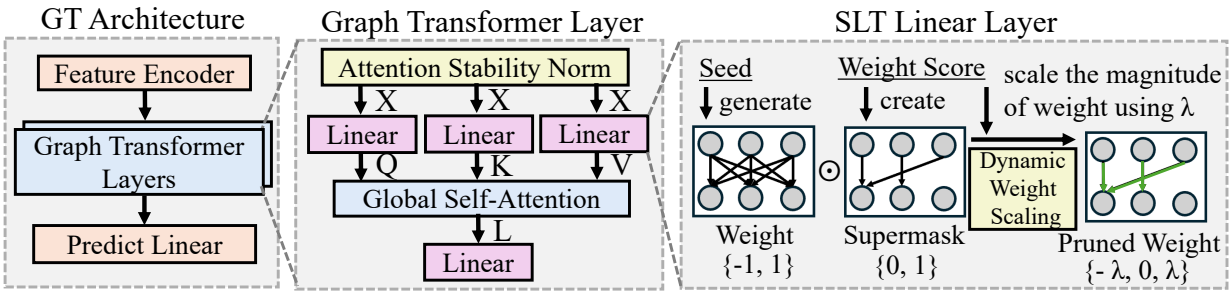

Figure 1: Overview of the Edge-Popup process using proposed Adaptive Scaling for Graph Transformers.

3.1 Preliminaries

Notation: In this paper, we adopt the following notational conventions: matrices are denoted by bold uppercase letters, $\mathbf{X}$, vectors by bold lowercase letters, $\mathbf{v}$, and scalars are written in regular lowercase letters, s. For the (i, j)-th element of a matrix $\mathbf{X}$, we use $\mathbf{X}_{ij}$. The graph's adjacency matrix is denoted as $\mathbf{A}$, while $\mathbf{X}$ represents the node feature matrix. Additionally, $\mathbf{W}$ refers to the weight matrix.

Graph Transformers: The architecture of GTs can be divided into two categories: pure GT, which does not include MPNNs, and hybrid GT, which does include MPNNs. This work uses NodeFormer and GRIT as pure GTs, and GraphGPS as a hybrid GT. NodeFormer utilizes a kernelized Gumbel-Softmax operator to enable efficient all-pair message passing, reducing the computational complexity from quadratic to linear. GRIT incorporates graph inductive biases without using message passing using learned relative positional encodings initialized with random walk probabilities. GraphGPS leverages positional and structural encoding for efficient node representation and uses both the MPNN layer and GT layer simultaneously

Graph Transformer calculates the attention score of each node in a graph by global self-attention mechanism:

$$\mathrm{Attn}(\mathbf{Q}, \mathbf{K}, \mathbf{V}) = \mathrm{Softmax}\left(\frac{\mathbf{Q}\mathbf{K}^{\mathrm{T}}}{\sqrt{d_k}}\right)\mathbf{V}, \tag{1}$$

$$\mathrm{Softmax}(z_i) = \frac{\exp(z_i)}{\sum_{j=1}^{N}\exp(z_j)}, \tag{2}$$

$$\mathbf{Q} = \mathbf{H}\mathbf{W}_Q, \quad \mathbf{K} = \mathbf{H}\mathbf{W}_K, \quad \mathbf{V} = \mathbf{H}\mathbf{W}_V, \tag{3}$$

where $\mathbf{H} \in \mathbb{R}^{N \times d_h}$ represents the hidden states of the nodes, and N is the number of nodes. $\mathbf{W}_Q, \mathbf{W}_K, \mathbf{W}_V \in \mathbb{R}^{d_h \times d_k}$ project the hidden states into the query, key, and value spaces, respectively. After global self-attention, the immediate results are further transformed through a linear projection with $\mathbf{W}_L$.

Edge-Popup: We follow the Edge-Popup (Ramanujan et al., 2020; Sreenivasan et al., 2022) to search for SLTs in linear layers. Each linear layer is assigned the same shape of learnable scores. These scores indicate the importance of the network connections and are used to generate the supermask by selecting the top-k% with the highest scores. Here, $k \in [0, 100]$ is a hyperparameter that controls the density of the supermask. Each element of the supermask m_{ij} is defined as:

$$m_{ij} = h(s_{ij}), \quad h(s_{ij}) = \begin{cases} 1, & |s_{ij}| \geq t \\ 0, & |s_{ij}| < t \end{cases}, \tag{4}$$

where s_{ij} is the element of weight score matrix, and $t \in \mathbb{R}^+$ is the threshold corresponding to the top k% of the absolute values in the weight scores. This implies that the SLT has a sparsity level of $(100 - k)$%.

The weights in the linear layers $(\mathbf{W}_Q, \mathbf{W}_K, \mathbf{W}_V, \mathbf{W}_L)$ are converted into an SLT format, denoted as $\mathbf{W}_{\mathrm{SLT}}$, and are obtained by:

$$\mathbf{W}_{\mathrm{SLT}} = \mathbf{W}_{\mathrm{rand}} \odot \mathbf{M}, \tag{5}$$

where $\mathbf{W}_{\mathrm{rand}} \in \{-1, 1\}^{m \times n}$ is a randomly initialized weight, and $\mathbf{M} \in \{0, 1\}^{m \times n}$ is the supermask for pruning.

3.2 Adaptive Scaling Strengthens SLTs

In this section, we show our approach to finding SLTs utilizing the Edge-Popup with our introduced Adaptive Scaling and evaluate its performance on accuracy to show its effectiveness.

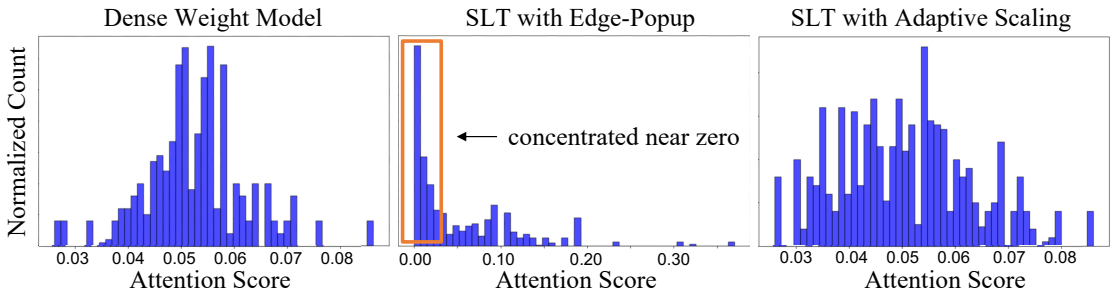

Figure 2: Comparing the attention score distributions between dense models and SLTs with and without Adaptive Scaling.

Edge-Popup fails in finding SLTs within GTs: We observe that *directly using Edge-Popup often fails to find accurate SLTs*, leading to worse accuracy in some datasets. Upon examining the distribution of attention scores, we observe that some node activations in the Softmax calculation become disproportionately large. As shown in Equation (2), when certain values of the Softmax input z_i are disproportionately large, the exponential term in the denominator causes other values to become extremely small, diminishing their contributions. As we explain below, a naive application of Edge-Popup often introduces such an imbalanced distribution of attention scores in GTs. As a result, these scores fail to provide meaningful attention to other nodes, leading to a distribution that deviates from an ideal form. This issue is particularly problematic in deep layer models, where the distribution imbalance accumulates layer by layer, destabilizing the scaling of activations. For example, when training GraphGPS on the CLUSTER dataset, we observed that in a 4-layer model, the accuracy difference between the dense model and SLT using Edge-Popup is 1%, 69.89% for the dense model and 68.49% for Edge-Popup. However, in a deeper 16-layer model, which is the recommended setting in their paper, the performance of Edge-Popup significantly deteriorates. The dense model achieves an accuracy of 78.02%, whereas the Edge-Popup model's accuracy drops drastically to 17.57%.

Unbalanced distribution of attention scores: Figure 2 illustrates a comparison of attention score distributions between dense models and SLT using Edge-Popup. The attention scores are distributed like a normal distribution in the dense model. In contrast, the SLT with Edge-Popup exhibits a distribution where most of the attention values are concentrated near zero, while a few values are significantly large. This indicates that the model assigns extreme attention to some nodes, disrupting the balanced aggregation across the graph.

We explore why some attention scores get excessively large. Dense models can dynamically adapt their weights through gradient descent to maintain balanced activations. In contrast, SLT weights obtained via Edge-Popup are randomly initialized and remain fixed during training, preventing the model from adjusting weight magnitudes to counteract imbalances in activations. The fixed nature of SLT weights leads to disproportionate activations in the attention mechanism, causing certain nodes to dominate the attention distribution. This imbalance accumulates across layers, undermining the representational capacity of the model.

To mitigate this imbalance, we propose *Adaptive Scaling*, which combines *Dynamic Weight Scaling* (DWS) and *Attention Stability Norm* (ASNorm). DWS allows us to control the scale of values within the attention computation, leading to a more balanced distribution across nodes, similar to the dense weight model. Additionally, we explore the ASNorm to support the stable search further, as detailed in the following sections.

Dynamic Weight Scaling: To address the imbalanced attention distribution observed in SLTs, we introduce a Dynamic Weight Scaling (DWS) approach that leverages the magnitude of weight scores during training. In the SLTH, weights are initialized randomly and remain fixed, which limits the adjustment of the magnitude of weights. Consequently, this restriction can lead to worse scaling of activations and hampers

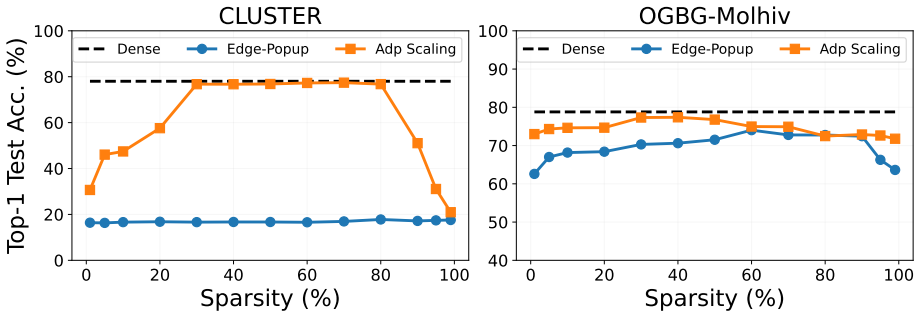

Figure 3: Results comparing SLT with and without Adaptive Scaling and Dense

SLT exploration. The DWS method uses a factor λ based on the absolute mean of the weight scores $\mathbf{S}$ and re-scales the weight matrix $\mathbf{W}_{\text{rand}}$ to produce new $\mathbf{W}_{\text{adp}}$. The process is shown in the following:

$$\mathbf{W}_{\text{adp}} = \frac{1}{mn} \sum_{i=1}^{m} \sum_{j=1}^{n} |\mathbf{S}_{ij}| \cdot \mathbf{W}_{\text{rand}} = \lambda \cdot \mathbf{W}_{\text{rand}}, \tag{6}$$

$$\mathbf{W}_{\text{SLT}} = \mathbf{W}_{\text{adp}} \odot \mathbf{M} = \lambda \cdot \mathbf{W}_{\text{rand}} \odot \mathbf{M}, \tag{7}$$

where m and n are the dimensions of the weight $\mathbf{W}$, score $\mathbf{S}$, and supermask $\mathbf{M}$.

In the Edge-popup algorithm, while weights remain fixed, the weight scores are updated dynamically through gradient descent. The pruning decision relies solely on the relative ranking of scores. However, by multiplying the weights with the absolute mean of the weight scores, we incorporate these scaling factors into the learning process, making it more adaptive than using only the relative rankings for pruning.

Attention Stability Norm: While DWS contributes to stabilizing attention distributions, we observed that the Attention Stability Norm (ASNorm) is necessary to further enhance training stability, particularly in deep layer models. In our SLT search, we incorporate PairNorm (Zhao & Akoglu, 2020), a normalization technique tailored for GNNs, to control the magnitude of node features effectively within each layer. PairNorm is designed to mitigate over-smoothing in MPNNs. It is achieved by maintaining a constant total pairwise feature distance across layers, which prevents node embeddings from becoming overly similar while preserving meaningful structural information. We also compare different normalization techniques, including BatchNorm (Ioffe & Szegedy, 2015), LayerNorm (Ba et al., 2016), and RMSNorm (Zhang & Sennrich, 2019), and find that PairNorm consistently provides the most stable and better results for SLT-based GTs in Table1.

Table 1: Comparing accuracy (%) across different normalization methods.

Normalization	PairNorm	BatchNorm	LayerNorm	RMSNorm	No Norm
CLUSTER	78.01	42.95	19.69	18.30	64.63
OGBG-Molhiv	74.01	66.86	68.03	67.08	73.13

Performance of Adaptive Scaling Figure 3 summarizes the results showing the accuracy of each configuration on the CLUSTER and OGBG-Molhiv datasets. The dense models achieve 78.02% and 78.80%, respectively, while SLT with Edge-Popup performs significantly worse at 17.57% and 74.03%. In contrast, our Adaptive Scaling enables SLTs to achieve accuracies close to the dense models, for instance, on CLUSTER reaches 77.41%. The effect of Adaptive Scaling is also illustrated in Figure 2 (right). These demonstrate that Adaptive Scaling effectively stabilizes attention distributions and enhances SLT performance.

Searching SLTs with DWS and ASNorm The pseudo-code of our SLT search algorithm is presented in Algorithm 1. It outlines the process for searching SLTs using the Edge-Popup with Adaptive Scaling (DWS and ASNorm).

Algorithm 1: Searching for SLTs within Graph Transformers using Adaptive Scaling

Input: Graph Transformer $g(\mathbf{A}, \mathbf{X}; \mathbf{W}_{\text{rand}})$, weight scores $\mathbf{S}$,
model sparsity s_T, learning rate γ, epochs T, ground truth labels $\mathbf{y}$
Output: $g(\mathbf{A}, \mathbf{X}_{\text{adp}}, \mathbf{W}_{\text{SLT}})$
Randomly initialize weights $\mathbf{W}_{\text{rand}}$ and scores $\mathbf{S}$ from seed
`# ASNorm: Normalize the Node embeddings`
$\mathbf{X}_{\text{adp}} \leftarrow \text{PairNorm}\,(\mathbf{X})$
for $t = 1$ ***to*** T **do**
  `# Get the threshold at top` s_T `by sorting` $\mathbf{S}$ `in descending order`
  $k_{\text{th}} \leftarrow \text{int}\,(\text{len}(\mathbf{S}) \times s_T)$
  $s_{\text{thres}} \leftarrow \text{sort}(|\mathbf{S}|)[k_{\text{th}}]$
  `# Generate the binary mask using` s_{thres}
  for *each element* $[i, j]$ ***in*** $\mathbf{S}$ **do**
    $\mathbf{M}[i, j] \leftarrow 0$ **if** $\mathbf{S}[i, j] < s_{\text{thres}}$ **else** 1
  `# DWS: scale the magnitude of weight`
  $\lambda \leftarrow \text{mean}(|\mathbf{S}|))$
  $\mathbf{W}_{\text{adp}} \leftarrow \lambda \cdot \mathbf{W}_{\text{rand}}$
  `# Pruning weight by element-wise multiplication with Supermask M`
  $\mathbf{W}_{\text{SLT}} \leftarrow \mathbf{W}_{\text{adp}} \odot \mathbf{M}$
  `# Update` $\mathbf{S}$ `from gradient`
  $\mathbf{S} \leftarrow \mathbf{S} - \gamma \nabla_{\mathbf{S}} \mathcal{L}(g(\mathbf{A}, \mathbf{X}_{\text{adp}}; \mathbf{W}_{\text{SLT}}, \mathbf{y})$
Return $g(\mathbf{A}, \mathbf{X}_{\text{adp}}, \mathbf{W}_{\text{SLT}})$

First, the weight matrix $\mathbf{W}_{\text{rand}}$ and the score matrix $\mathbf{S}$ are randomly initialized using a random seed. Second, the node embeddings $\mathbf{X}$ are normalized using PairNorm to stabilize searching. Third, the algorithm iterates over T epochs to search for the accurate subnetworks with sparsity level s_T. In each epoch, the threshold s_{thres} corresponding to the top s_T fraction of absolute values in $\mathbf{S}$ is computed. A binary supermask $\mathbf{M}$ is generated by setting $M_{ij} = 1$ if $|S_{ij}| \geq S_{\text{thres}}$ and $M_{ij} = 0$ otherwise. Dynamic weight scaling is applied by calculating the scaling factor $\lambda = \text{mean}(|\mathbf{S}|)$ and updating the weights as $\mathbf{W}_{\text{adp}} = \lambda \cdot \mathbf{W}_{\text{rand}}$. The sparse model weights are obtained by element-wise multiplying $\mathbf{W}_{\text{adp}}$ with the supermask $\mathbf{M}$, resulting in $\mathbf{W}_{\text{SLT}} = \mathbf{W}_{\text{adp}} \odot \mathbf{M}$. Finally, the score matrix $\mathbf{S}$ is updated using gradient descent on the loss function $\mathcal{L}$ computed with $\mathbf{W}_{\text{SLT}}$.

In this study, we search for SLTs by applying supermask to the weights, as shown in Equation (5). We have modified the linear projection components within the GT layers, which are the primary layers utilizing the self-attention mechanism. In other words, we can search for SLTs without modifying the attention mechanisms themselves, making them flexible enough to fit any GT architecture. We apply the supermask to all linear projection layers in the Transformer layer, not only to the Query, Key, and Value matrix of the self-attention but also to the weights in the feed-forward networks.

4 Experiments and Results

This section describes experiments using several Graph Transformers (GTs) architectures and datasets to assess the performance of the SLTs. We analyze the effectiveness, in particular, in the robustness toward perturbations and out-of-distribution (OOD) detection, which are considered a challenge in GTs. We also show memory reduction of SLTs compared with dense weight learning models.

Baseline Architectures: We use three popular models to validate that SLTs exist in versatile GT architectures. The first one is NodeFormer (Wu et al., 2022a), a pure GT designed for node-level classification in

large graphs. The second one, GRIT (Ma et al., 2023), is a pure GT for graph-level tasks. The third one, GraphGPS (Rampášek et al., 2022), is a hybrid GT that combines both local message passing and global attention mechanisms for graph-level tasks. Our experiments basically follow the configurations (the number of layers, etc.) and hyperparameters of their original papers, with adjustments to the learning rate and SLT sparsity.

Datasets: We use the same datasets as in the original papers to ensure a fair comparison. For NodeFormer, we use seven tasks from Cora, Citeseer, Pubmed (Sen et al., 2008), Deezer (Rozemberczki & Sarkar, 2020), Actor (Pei et al., 2020), Mini-ImageNet (Vinyals et al., 2016) and 20News-Groups (Pedregosa et al., 2011). Cora, Citeseer, and Pubmed are citation networks, Deezer and Actor are social networks, Mini-ImageNet is an image classification, and 20News-Groups is a text classification task. For GRIT and GraphGPS, we use five tasks, ZINC, MNIST, CIFAR10, PATTERN, and CLUSTER, from Benchmarking GNNs (Dwivedi et al., 2023), and OGBG-Molhiv from Open Graph Benchmark (OGB) (Hu et al., 2020). ZINC is the molecular regression task, MNIST and CIFAR10 are the image classification tasks, and PATTERN and CLUSTER are synthetic datasets sampled from the stochastic block model. OGBG-Molhiv is designed for molecular property prediction. The details of the datasets used are provided in Appendix A.

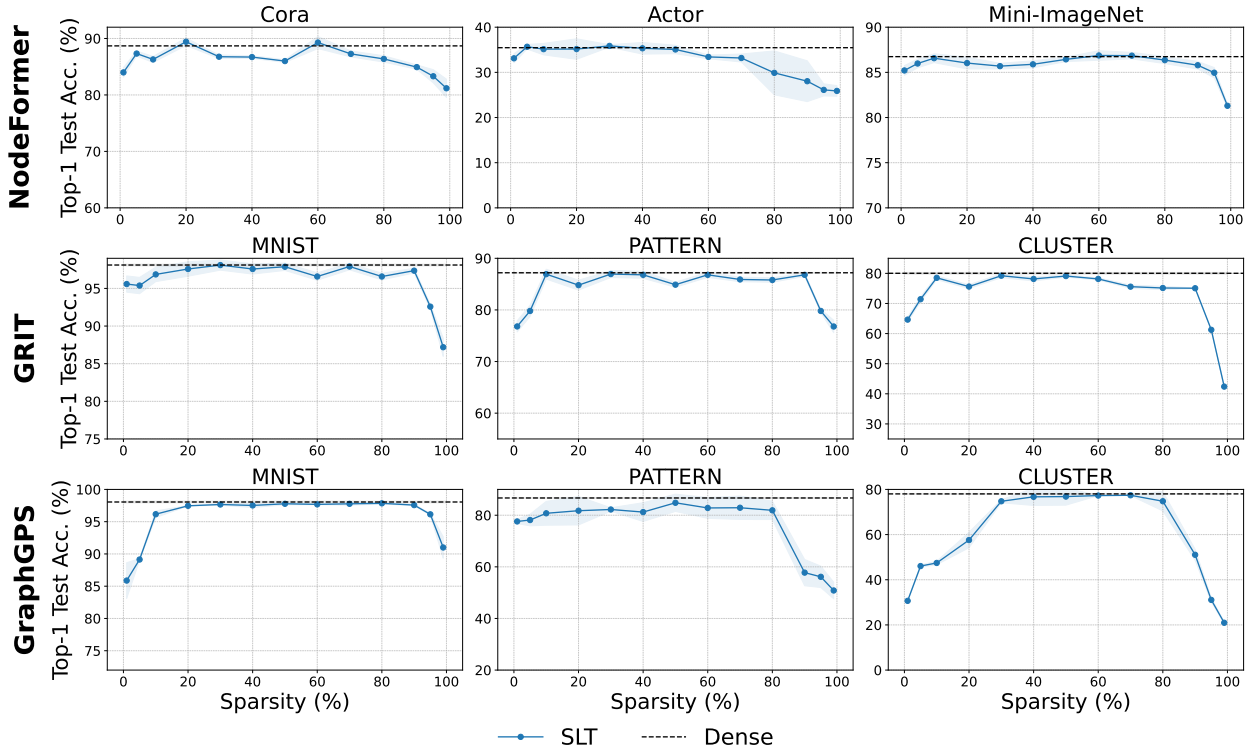

Figure 4: Comparison of the accuracy of SLTs and dense weight learning models across varying sparsity levels in different GT architectures and datasets. The top row corresponds to NodeFormer evaluated on the Cora, Actor, and Mini-ImageNet datasets. The middle row presents GRIT's performance on MNIST, PATTERN, and CLUSTER datasets, while the bottom row shows GraphGPS evaluated on the same datasets. The results demonstrate that SLTs achieve accuracy comparable to dense models across a wide range of sparsity levels (10% to 90%).

4.1 Accuracy benchmarking on SLTs

In Figure 4, we plot accuracy against sparsity (1% $\sim$ 99%) for SLTs in the three architectures. In the NodeFormer on Cora, the dense model achieves an accuracy of 88.69%, while the SLT with 60% sparsity attains a higher accuracy of 89.42%. At very low (<10%) and very high (>90%) sparsity levels, accuracy

drops considerably (e.g., accuracy decreases to 81.18% at 99% sparsity on Cora). Across these architectures, we observe that SLT peaks within a moderate sparsity range (10% to 90%), aligning closely with or surpassing dense models' performance.

4.2 Accuracy-to-Size Trade-off

Memory efficiency is a critical challenge for GTs, given their high computational and memory demands. Figure 5 further illustrates the significant improvements achieved in the trade-off between accuracy and memory. SLTs consistently achieve similar or superior accuracy reducing memory demands compared to the dense models. This steep improvement at lower memory levels demonstrates how SLTs enable GTs to perform effectively even in highly resource-constrained environments, making them well-suited for deployment on edge devices or other memory-limited systems.

Table 2 compares NodeFormer-SLT with NodeFormer-Dense, traditional MPNN models GCN and GAT. It shows that NodeFormer-SLT achieves the highest accuracy (78.20%) while consuming only 0.619 MB of memory—significantly less than NodeFormer-Dense (4.512 MB), GCN (0.982 MB), or GAT (0.982 MB). These are all two-layer architectures. This demonstrates the effectiveness of SLTs in drastically reducing memory usage while maintaining or even improving model performance compared to both dense GTs and MPNNs.

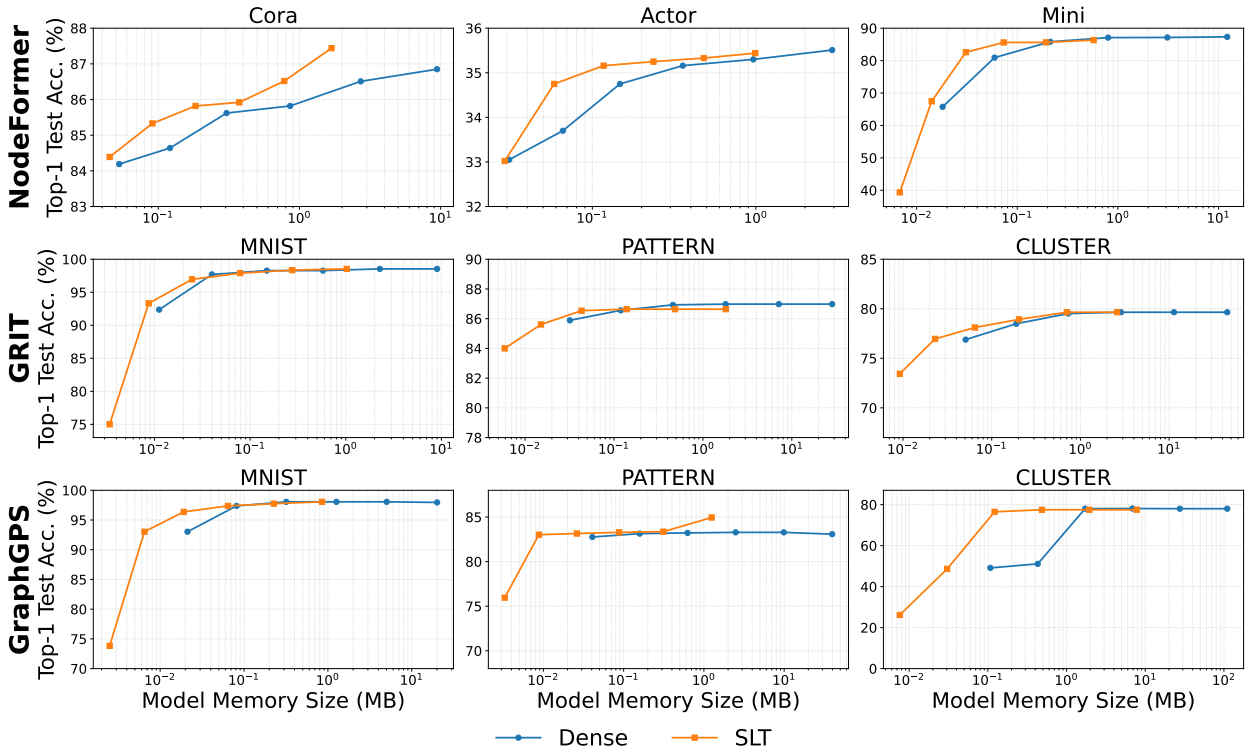

Figure 5: Comparison of the trade-off between model memory usage and accuracy for SLT and dense weight learning models. The hidden channels are varied across values of 8, 16, 32, 64, 128, and 256. This figure illustrates that the SLT model significantly improves the trade-off, achieving high accuracy while substantially reducing memory consumption compared to the dense model.

4.3 Out-of-distribution (OOD) data detection

In this section, we compare the generalization of SLTs in GTs by evaluating the ability to detect and manage OOD instances against dense models. A key indicator of model robustness, particularly in real-world scenarios, is its performance on OOD data, *i.e.* data that present patterns or characteristics unseen

Table 2: Comparison of memory usage and accuracy across different models on Pubmed datasets (2-layer, 256 hidden channels) with NodeFormer (SLT, Dense), GCN, and GAT.

	NodeFormer-SLT	**NodeFormer-Dense**	**GCN**	**GAT**
Memory (MB)	0.619 ($\times$7.3 $\downarrow$)	4.512	0.982	0.982
Accuracy (%)	78.20	75.54	75.98	76.4

during training. It is often critical for real-world applications of GTs, as they can process graphs with new or unexpected structures, potentially leading to performance degradation if the model overfits the training data distributions. Our experiments utilize OOD test sets across various tasks to evaluate to what extent SLTs can generalize beyond the training data distribution.

To evaluate OOD detection performance, we used ROC-AUC as the primary metric. As shown in Figure 6, SLTs respond more robustly to OOD data, achieving higher detection rates and better classification stability than dense models. For instance, SLTs improve accuracy by approximately 0.15 to 0.4 on the Cora dataset, 0.2 to 0.3 on Citeseer, and 0.05 to 0.2 on Actor. These gains likely stem from the inherent regularization effects of SLTs, which help mitigate overfitting and maintain performance on unseen data distributions. By enforcing sparsity, SLTs focus on the most salient features and connections, improving generalization to OOD data. Consequently, SLTs enhance OOD robustness, contributing to greater model reliability and safety in critical applications.

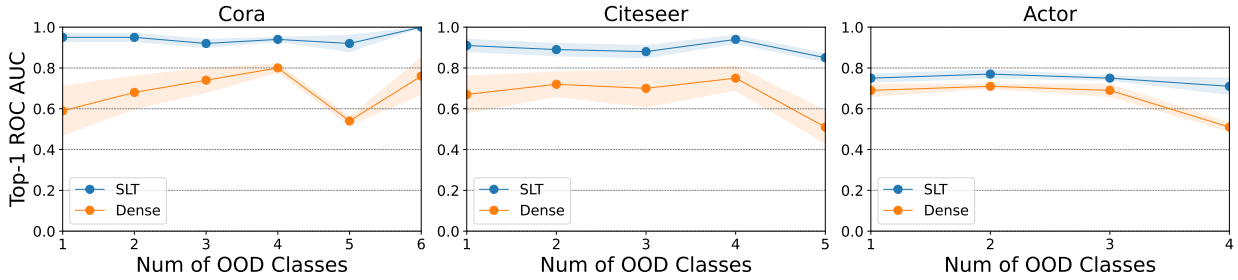

Figure 6: Performance comparison on OOD data between SLT and dense models, evaluated by ROC-AUC. The x-axis represents the number of OOD classes randomly selected from the dataset classes. During training, OOD classes were removed, and the models were tested on their ability to detect these unseen classes.

4.4 Perturbation

Real-world graph data often contains noise or errors, making robustness to perturbations critical for reliable performance. Perturbations typically occur in two forms: node perturbations, where noise is added to node features (e.g., due to sensor inaccuracies or incomplete information), and edge perturbations, which modify graph connections to simulate errors or dynamic changes in relationships. By assessing both types, we evaluate the robustness of SLTs compared to dense models, highlighting their ability to handle noisy inputs and structural modifications effectively.

Node Perturbation: We examine the robustness of SLTs under node perturbations by adding Gaussian noise to node features during inference and simulating common real-world scenarios such as noisy sensor data or incomplete information in social networks.

The perturbation is applied to each node feature by adding Gaussian noise with strength controlled by a factor ϵ. The perturbed feature $\tilde{x}$ is given by:

$$\tilde{x} = x + z, \quad z \sim \mathcal{N}(0, \epsilon^2), \tag{8}$$

where x is the element of original node feature, and z is sampled from a standard normal distribution. Since z scales the noise by ϵ, $\tilde{x}$ retains a Gaussian distribution with mean 0 and variance ϵ^2.

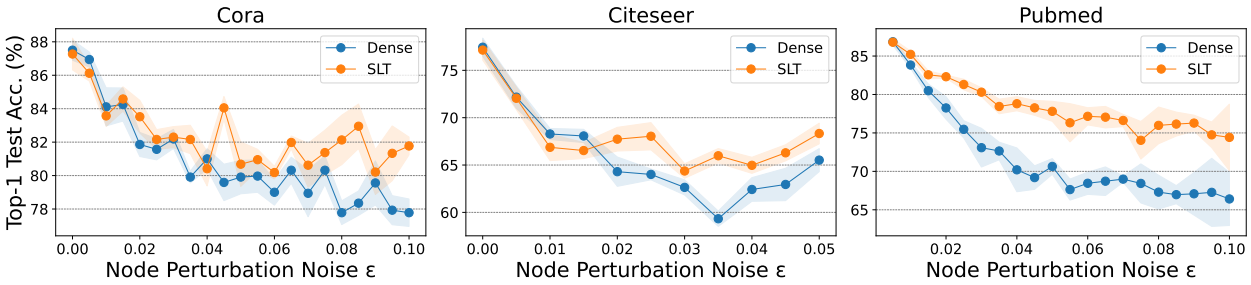

Figure 7: Classification accuracy of SLTs and dense models under varying levels of node feature perturbation on the Cora, Citeseer, and Pubmed datasets. Gaussian noise with standard deviation ϵ is added to the node features to simulate node perturbation.

The results, presented in Figure 7, indicate that SLTs outperform dense models even under high noise levels, maintaining stable accuracy as ϵ increases up to a certain threshold. Specifically, on the Cora dataset, SLTs achieve a 1% to 5% improvement when ϵ exceeds 0.04. For Citeseer, SLTs show around a 5% improvement starting from $\epsilon = 0.02$. On Pubmed, SLTs demonstrate robustness even at small ϵ, with a gradual increase in performance and up to a 10% improvement under higher noise levels. This robustness suggests that the sparsity introduced in SLTs acts as a form of regularization, reducing model complexity and preventing overfitting to noise-free training data. By focusing on the most critical connections, SLTs may enhance the ability to generalize to perturbed inputs, leading to improved robustness against noise.

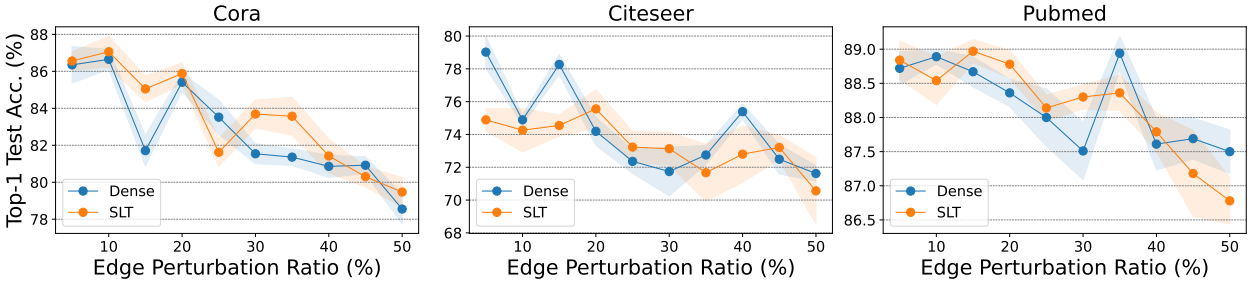

Figure 8: Classification accuracy of SLTs and fully trained dense models under varying levels of edge perturbation on benchmark datasets. Edge perturbation is performed by randomly reassigning a certain percentage of edges to different destination nodes.

Edge Perturbation: In addition to node feature perturbation, we test the robustness of SLTs under edge perturbation. This process simulates real-world situations where relational data might be incomplete or contain erroneous connections, such as in dynamic or evolving networks. The edge perturbation process involves selecting a subset of edges and replacing each edge's destination node with a random alternative node during inference, controlled by a parameter representing the percentage of edges modified.

As shown in Figure 8, SLTs do not exhibit a distinct advantage over dense models under edge perturbation. This result stems from a key characteristic of GTs: unlike MPNN, they do not rely on direct edge connections for information aggregation. Instead, graph structure, including edges, is often encoded as part of the node features in the preprocessing stage or used as a supplementary factor in the aggregation process. In other words, SLTs have the least effect on edges or graph structure. Therefore, while SLTs exhibit significant robustness under node perturbation, they do not confer a comparable robustness advantage under structural modifications like edge perturbation.

5 Limitations and Future Works

Our proposed SLT approach has shown considerable benefits in reducing memory consumption and improving robustness in GTs. However, there are several limitations and promising directions for future research.

Extension to a broader range of applications: While we have demonstrated the effectiveness of SLTs in GTs for node- and graph-level tasks, extending our findings to a wider variety of graph types and applications—such as link prediction and graph generation—would help further validate the versatility and scalability of our method.

Large-scale graphs: In extremely large-scale graphs, techniques such as sparse attention mechanisms or graph partitioning are commonly used. In these cases, the global scope of the attention mechanism is explicitly reduced, as the computation that originally considered all node pairs may be limited to a smaller subset. Investigating the combination of SLT with these techniques, particularly when the perceptual scope decreases, will help us understand whether SLT can still be effective. This can lead to more efficient acceleration for large-scale graphs.

Unstructured or structural pruning: Our method, as well as the majority of other SLTH-based approaches, employs an unstructured pruning approach. However, structural pruning is often preferred in hardware like GPUs, as it can improve resource utilization and, thus, the inference speed, while it potentially impacts accuracy. It is worth exploring the trade-off between unstructured and structural pruning with constraints on both accuracy and memory size.

6 Conclusion

In this paper, we explored the existence of SLTs within GTs and highlighted their effectiveness in addressing key challenges, such as high memory consumption, lack of robustness to perturbations, and limited generalization to OOD data.

- We provide the first empirical evidence of the existence of SLTs within GTs, demonstrating their applicability across both pure and hybrid GT architectures.
- We identify that traditional SLT methods can fail to find SLTs within GTs, so we introduce Adaptive Scaling, a novel technique that balances attention distributions and improves search stability.
- Our findings show that SLTs significantly reduce memory consumption, achieving up to $32\times$ reduction while maintaining or even outperforming the accuracy of fully trained dense models. Furthermore, the proposed SLT method enhances robustness against adversarial perturbations and enhances generalization to OOD data, ensuring model reliability in real-world scenarios.

References

Jimmy Lei Ba, Jamie Ryan Kiros, and Geoffrey E. Hinton. Layer normalization. *arXiv preprint arXiv:1607.06450*, 2016.

Chiho Choi, Joon Hee Choi, Jiachen Li, and Srikanth Malla. Shared cross-modal trajectory prediction for autonomous driving. In *Proceedings of the IEEE/CVF Conference on Computer Vision and Pattern Recognition*, pp. 244–253, 2021.

Francesco Di Giovanni, Lorenzo Giusti, Federico Barbero, Giulia Luise, Pietro Lio, and Michael M. Bronstein. On over-squashing in message passing neural networks: The impact of width, depth, and topology. In *Proceedings of the 40th International Conference on Machine Learning*, pp. 7865–7885. PMLR, 2023.

Vijay Prakash Dwivedi, Chaitanya K Joshi, Anh Tuan Luu, Thomas Laurent, Yoshua Bengio, and Xavier Bresson. Benchmarking graph neural networks. *Journal of Machine Learning Research*, 24(43):1–48, 2023.

Wenqi Fan, Yao Ma, Qing Li, Yuan He, Eric Zhao, Jiliang Tang, and Dawei Yin. Graph neural networks for social recommendation. In *The world wide web conference*, pp. 417–426, 2019.

Philipp Foth, Lukas Gosch, Simon Geisler, Leo Schwinn, and Stephan Günnemann. Relaxing graph transformers for adversarial attacks. *arXiv preprint arXiv:2407.11764*, 2024.

Jonathan Frankle and Michael Carbin. The lottery ticket hypothesis: Finding sparse, trainable neural networks. In *International Conference on Learning Representations*, 2019.

Chen Gao, Xiang Wang, Xiangnan He, and Yong Li. Graph neural networks for recommender system. In *Proceedings of the fifteenth ACM international conference on web search and data mining*, pp. 1623–1625, 2022.

Ángel López García-Arias, Yasuyuki Okoshi, Masanori Hashimoto, Masato Motomura, and Jaehoon Yu. Recurrent residual networks contain stronger lottery tickets. *IEEE Access*, 11:16588–16604, 2023. doi: 10.1109/ACCESS.2023.3245808.

Thomas Gaudelet, Ben Day, Arian R Jamasb, Jyothish Soman, Cristian Regep, Gertrude Liu, Jeremy BR Hayter, Richard Vickers, Charles Roberts, Jian Tang, et al. Utilizing graph machine learning within drug discovery and development. *Briefings in bioinformatics*, 22(6):bbab159, 2021.

Weihua Hu, Matthias Fey, Marinka Zitnik, Yuxiao Dong, Hongyu Ren, Bowen Liu, Michele Catasta, and Jure Leskovec. Open graph benchmark: Datasets for machine learning on graphs. *Advances in neural information processing systems*, 33:22118–22133, 2020.

Tianjin Huang, Tianlong Chen, Meng Fang, Vlado Menkovski, Jiaxu Zhao, Lu Yin, Yulong Pei, Decebal Constantin Mocanu, Zhangyang Wang, Mykola Pechenizkiy, and Shiwei Liu. You can have better graph neural networks by not training weights at all: Finding untrained gnns tickets. In *Proceedings of the First Learning on Graphs Conference*, volume 198, pp. 8:1–8:17. PMLR, 2022.

Sergey Ioffe and Christian Szegedy. Batch normalization: accelerating deep network training by reducing internal covariate shift. In *Proceedings of the 32nd International Conference on International Conference on Machine Learning - Volume 37*, ICML'15, pp. 448–456. JMLR.org, 2015.

Weiwei Jiang and Jiayun Luo. Graph neural network for traffic forecasting: A survey. *Expert systems with applications*, 207:117921, 2022.

Thomas N. Kipf and Max Welling. Semi-supervised classification with graph convolutional networks. In *International Conference on Learning Representations*, 2017.

Eugene Ku. Stronger graph transformer with regularized attention scores. *arXiv preprint arXiv:2312.11730*, 2023.

Adam Lerer, Ledell Wu, Jiajun Shen, Timothee Lacroix, Luca Wehrstedt, Abhijit Bose, and Alex Peysakhovich. Pytorch-biggraph: A large scale graph embedding system. *Proceedings of Machine Learning and Systems*, 1:120–131, 2019.

Qimai Li, Zhichao Han, and Xiao-Ming Wu. Deeper insights into graph convolutional networks for semi-supervised learning. In *Proceedings of the AAAI conference on artificial intelligence*, volume 32, 2018.

Zenan Li, Qitian Wu, Fan Nie, and Junchi Yan. Graphde: A generative framework for debiased learning and out-of-distribution detection on graphs. *Advances in Neural Information Processing Systems*, 35: 30277–30290, 2022.

Liheng Ma, Chen Lin, Derek Lim, Adriana Romero-Soriano, Puneet K Dokania, Mark Coates, Philip Torr, and Ser-Nam Lim. Graph inductive biases in transformers without message passing. In *International Conference on Machine Learning*, pp. 23321–23337. PMLR, 2023.

Eran Malach, Gilad Yehudai, Shai Shalev-Schwartz, and Ohad Shamir. Proving the lottery ticket hypothesis: Pruning is all you need. In *Proceedings of the 37th International Conference on Machine Learning*, pp. 6682–6691. PMLR, 2020.

Yasuyuki Okoshi, Ángel López García-Arias, Kazutoshi Hirose, Kota Ando, Kazushi Kawamura, Thiem Van Chu, Masato Motomura, and Jaehoon Yu. Multicoated supermasks enhance hidden networks. In *Proceedings of the 39th International Conference on Machine Learning*, pp. 17045–17055. PMLR, 2022.

Kenta Oono and Taiji Suzuki. Graph neural networks exponentially lose expressive power for node classification. In *International Conference on Learning Representations*, 2020.

Laurent Orseau, Marcus Hutter, and Omar Rivasplata. Logarithmic pruning is all you need. *Advances in Neural Information Processing Systems*, 33:2925–2934, 2020.

Hikari Otsuka, Daiki Chijiwa, Ángel López García-Arias, Yasuyuki Okoshi, Kazushi Kawamura, Thiem Van Chu, Daichi Fujiki, Susumu Takeuchi, and Masato Motomura. Partial search in a frozen network is enough to find a strong lottery ticket. *arXiv preprint arXiv:2402.14029*, 2024.

Fabian Pedregosa, Gaël Varoquaux, Alexandre Gramfort, Vincent Michel, Bertrand Thirion, Olivier Grisel, Mathieu Blondel, Peter Prettenhofer, Ron Weiss, Vincent Dubourg, Jake Vanderplas, Alexandre Passos, David Cournapeau, Matthieu Brucher, Matthieu Perrot, and Édouard Duchesnay. Scikit-learn: Machine learning in python. *Journal of Machine Learning Research*, 12(85):2825–2830, 2011.

Hongbin Pei, Bingzhe Wei, Kevin Chen-Chuan Chang, Yu Lei, and Bo Yang. Geom-GCN: Geometric graph convolutional networks. In *International Conference on Learning Representations*, 2020.

Ankit Pensia, Shashank Rajput, Alliot Nagle, Harit Vishwakarma, and Dimitris Papailiopoulos. Optimal lottery tickets via subset sum: Logarithmic over-parameterization is sufficient. *Advances in neural information processing systems*, 33:2599–2610, 2020.

Vivek Ramanujan, Mitchell Wortsman, Aniruddha Kembhavi, Ali Farhadi, and Mohammad Rastegari. What's hidden in a randomly weighted neural network? In *Proceedings of the IEEE/CVF Conference on Computer Vision and Pattern Recognition*, pp. 11893–11902, 2020.

Ladislav Rampášek, Mikhail Galkin, Vijay Prakash Dwivedi, Anh Tuan Luu, Guy Wolf, and Dominique Beaini. Recipe for a general, powerful, scalable graph transformer. In *Advances in Neural Information Processing Systems*, volume 35, pp. 18948–18963, 2022.

Benedek Rozemberczki and Rik Sarkar. Characteristic functions on graphs: Birds of a feather, from statistical descriptors to parametric models. In *Proceedings of the 29th ACM International Conference on Information and Knowledge Management*, pp. 1325–1334. ACM, 2020.

Prithviraj Sen, Galileo Namata, Mustafa Bilgic, Lise Getoor, Brian Galligher, and Tina Eliassi-Rad. Collective classification in network data. *AI Magazine*, 29(3):93–106, 2008.

Kartik Sreenivasan, Jy-yong Sohn, Liu Yang, Matthew Grinde, Alliot Nagle, Hongyi Wang, Eric Xing, Kangwook Lee, and Dimitris Papailiopoulos. Rare gems: Finding lottery tickets at initialization. *Advances in neural information processing systems*, 35:14529–14540, 2022.

Jake Topping, Francesco Di Giovanni, Benjamin Paul Chamberlain, Xiaowen Dong, and Michael M. Bronstein. Understanding over-squashing and bottlenecks on graphs via curvature. *International Conference on Learning Representations*, 2022.

Oriol Vinyals, Charles Blundell, Timothy Lillicrap, Daan Wierstra, et al. Matching networks for one shot learning. *Advances in neural information processing systems*, 29, 2016.

Qitian Wu, Wentao Zhao, Zenan Li, David Wipf, and Junchi Yan. Nodeformer: A scalable graph structure learning transformer for node classification. In *Advances in Neural Information Processing Systems*, 2022a.

Qitian Wu, Yiting Chen, Chenxiao Yang, and Junchi Yan. Energy-based out-of-distribution detection for graph neural networks. In *International Conference on Learning Representations*, 2023.

Shiwen Wu, Fei Sun, Wentao Zhang, Xu Xie, and Bin Cui. Graph neural networks in recommender systems: A survey. *ACM Computing Surveys*, 55(5):1–37, 2022b.

Rui Xue, Haoyu Han, Mohamadali Torkamani, Jian Pei, and Xiaorui Liu. LazyGNN: Large-scale graph neural networks via lazy propagation. In *Proceedings of the 40th International Conference on Machine Learning*, pp. 38926–38937. PMLR, 2023.

Jiale Yan, Hiroaki Ito, Ángel López García-Arias, Yasuyuki Okoshi, Hikari Otsuka, Kazushi Kawamura, Thiem Van Chu, and Masato Motomura. Multicoated and folded graph neural networks with strong lottery tickets. In *Learning on Graphs Conference*, pp. 11–1. PMLR, 2024.

Biao Zhang and Rico Sennrich. Root mean square layer normalization. *Advances in Neural Information Processing Systems*, 32, 2019.

Xiang Zhang, Marko Zeman, Theodoros Tsiligkaridis, and Marinka Zitnik. Graph-guided network for irregularly sampled multivariate time series. In *International Conference on Learning Representations*, 2022.

Lingxiao Zhao and Leman Akoglu. Pairnorm: Tackling oversmoothing in gnns. In *International Conference on Learning Representations*, 2020.

Hattie Zhou, Janice Lan, Rosanne Liu, and Jason Yosinski. Deconstructing lottery tickets: Zeros, signs, and the supermask. In *Advances in Neural Information Processing Systems*, pp. 3592–3602, 2019.

Xiao Zhou, Weizhong Zhang, Hang Xu, and Tong Zhang. Effective sparsification of neural networks with global sparsity constraint. In *Proceedings of the IEEE/CVF Conference on Computer Vision and Pattern Recognition*, pp. 3599–3608, 2021.

Yonghua Zhu, Jincheng Huang, Yang Chen, Robert Amor, and Michael Witbrock. A graph transformer defence against graph perturbation by a flexible-pass filter. *Information Fusion*, 107:102296, 2024.

Appendix

A Datasets

For node-level prediction: We use seven datasets Cora, Citeseer, Pubmed, Deezer, Actor, Mini-ImageNet, and 20News-Groups. The Cora, Citeseer, and Pubmed datasets are citation network datasets where each document is represented as a node, and each citation link between documents serves as an edge. Deezer is a social network of users from European countries on the Deezer platform, where edges show mutual follower relationships. The features for each node come from the artists each user likes, and nodes are labeled with gender. The Actor dataset is a graph of actors appearing together on Wikipedia pages. Each node is an actor, and an edge between two nodes means both actors were mentioned on the same Wikipedia page. The 20News dataset contains around 20,000 documents from newsgroups, organized (almost) equally across 20 different groups, with each document represented as a node. The Mini-ImageNet dataset comprises 84x84 RGB images, covering 100 classes with 600 images in each class.

For graph-level prediction: We use six datasets ZINC, MNIST, CIFAR10, PATTERN, CLUSTER, and OGBG-Molhiv. ZINC is 12,000 molecular graphs from the ZINC database, tasked with regressing constrained solubility (logP) values. CIFAR10 and MNIST are image datasets from SLIC superpixels from 8-nearest-neighbor graphs for 10-class classification. PATTERN is a synthetic dataset using Stochastic Block Models to classify nodes into one of 100 subgraph patterns. CLUSTER is a synthetic dataset of graphs with six SBM-generated clusters, aiming to classify nodes by cluster-ID. OGBG-Molhiv is a molecular property dataset for binary classification of a molecule's ability to inhibit HIV replication.

B Supplementary Experimental Results

Experiments evaluate for NodeFormer on Cora, Citeseer, Pubmed, Deezer, Actor, Mini-ImageNet, and 20News-Groups, for GRIT and GraphGPS on ZINC, MNIST, CIFAR10, PATTERN, CLUSTER, and OGBG-Molhiv. We compare SLT performance with the fully trained dense model in Table 4 5.

Table 3: Overview of the graph dataset used in this study.

DataSets	**#Graphs**	**Avg. #Nodes**	**Avg. #Edges**	**#Node Feat**	**#Classes**	**Metric**
Cora	1	2,708	5,429	1,433	7	Accuracy
Citeseer	1	3,327	4,732	3,703	6	Accuracy
Pubmed	1	19,717	88,648	500	3	Accuracy
Deezer	1	28,281	92,752	31,241	2	ROC-AUC
Actor	1	7,600	29,926	931	5	Accuracy
Mini-ImageNet	1	18,000	0	128	30	Accuracy
20News-Groups	1	9,607	0	236	10	Accuracy
ZINC	12,000	23.2	24.9	1	0	MAE
MNIST	70,000	70.6	564.5	3	10	Accuracy
CIFAR10	60,000	117.6	941.1	5	10	Accuracy
PATTERN	14,000	118.9	3,039.3	3	2	Accuracy
CLUSTER	12,000	117.2	2,150.9	7	6	Accuracy
OGBG-Molhiv	41,127	25.5	27.5	9	2	ROC-AUC

Table 4: Experiments comparison accuracy between fully trained dense model and SLT of NodeFormer on six benchmark datasets.

Datasets	**Cora**	**Citeseer**	**Deezer**	**Actor**	**Mini-ImageNet**	**20News-Groups**
NodeFormer-Dense	88.69 ± 0.46	76.33 ± 0.59	71.24 ± 0.32	35.31 ± 1.29	86.74 ± 0.23	65.21 ± 1.14
NodeFormer-SLT	89.42 ± 0.56	76.93 ± 1.30	72.96 ± 0.48	37.62 ± 0.40	87.21 ± 0.54	65.60 ± 0.38

Table 5: Experiments comparison accuracy between fully trained dense model and SLT of GRIT and GraphGPS on five benchmark datasets.

Datasets	**ZINC**	**MNIST**	**CIFAR10**	**PATTERN**	**CLUSTER**
	MAE ↓	Accuracy ↑	Accuracy ↑	Accuracy ↑	Accuracy ↑
GRIT-Dense	0.059 ± 0.002	98.10 ± 0.111	76.468 ± 0.881	87.196 ± 0.076	80.026 ± 0.277
GRIT-SLT	0.077 ± 0.005	98.10 ± 0.324	71.36 ± 0.37	86.95 ± 0.51	79.22 ± 0.42
GraphGPS-Dense	0.070 ± 0.004	98.051 ± 0.126	72.298 ± 0.356	86.685 ± 0.059	78.016 ± 0.180
GraphGPS-SLT	0.098 ± 0.014	97.980 ± 0.153	72.460 ± 0.422	83.941 ± 0.272	77.501 ± 0.251